[CANCER RESEARCH 57, 1682–1689, May 1, 1997]

Urokinase-Type Plasminogen Activator Receptors Associate with β_1 and β_3 Integrins of Fibrosarcoma Cells: Dependence on Extracellular Matrix Components[1]

Wei Xue, Ikuko Mizukami, Robert F. Todd III, and Howard R. Petty[2]

Department of Biological Sciences, Wayne State University, Detroit, Michigan 48202 [W. X., H. R. P.], and Department of Internal Medicine, University of Michigan Medical School, Ann Arbor, Michigan 48109 [I. M., R. F. T.]

ABSTRACT

We have shown previously that the urokinase-type plasminogen activator receptor (uPAR) physically associates with β_2 integrins on human leukocyte membranes. We now report that uPAR associates with certain members of the β_1 and β_3 integrin families expressed by a nonhematopoietic fibrosarcoma cell line (HT1080) when adherent to certain extracellular matrix molecules. Flow cytometry studies indicated that HT1080 cells expressed uPAR and β_1 and β_3 integrins. Double staining immunofluorescence was used to label uPAR and β_1 and β_3 integrins. The staining patterns of uPAR and β_1 integrins were strikingly similar when attached to fibronectin, laminin, or vitronectin but not polylysine-coated substrates. Resonance energy transfer (RET) between uPAR and β_1 integrins was observed, especially at focal adhesion plaques; this indicates that these molecules are within about 7 nm of each other on these cell membranes. uPAR and β_3 integrin coclustering and RET were also observed on tumor cells adherent to vitronectin but not to fibronectin, laminin, or polylysine-coated surfaces. Because *N*-acetyl-D-glucosamine was found previously to inhibit β_2 integrin-uPAR association, we tested the effect of saccharides on the β_1-uPAR and β_3-uPAR colocalization and RET. Colocalization and RET between uPAR and β_1 or β_3 integrins were effectively inhibited by *N*-acetyl-D-glucosamine on extracellular matrix-coated surfaces. To better define which members of β_1 and β_3 integrin families associate with uPAR, we studied the association of several α subunits with uPAR on tumor cells. We found that: (*a*) α_5 colocalizes with uPAR on cells attached to fibronectin-coated surfaces; (*b*) α_5 and α_v colocalize with uPAR on cells adherent to vitronectin; and (*c*) α_3 and α_6 associate with uPAR on cells attached to laminin. In further support of physical associations between integrins and uPAR on tumor cells, uPAR was found to coimmunoprecipitate with β_1 integrins in Brij-58 lysates of HT1080 cells (as detected by anti-uPAR Western blotting of material isolated from an anti-β_1 integrin immunoaffinity column). Thus, uPAR may laterally associate with integrins of tumor cells when attached to specific extracellular matrix elements to enable directional proteolysis for tumor cell migration and invasion.

INTRODUCTION

Malignant tumor cells invade surrounding tissues by penetrating basement membranes, connective tissues, and cellular planes (1–3). Subsequent metastasis requires distribution via the lymphatic or blood circulatory systems, followed by extravasation and invasion. The invasive program of malignant cells requires the complex interplay of various cell surface molecules participating in adhesion, detachment, and proteolytic disruption of neighboring structures (1–6). Thus, tumor cells coordinate the complementary functions of cell-cell/cell-matrix adherence and pericellular proteolysis to promote invasion. Two membrane components participating in the regulation of adherence phenomena and proteolysis are integrins and uPARs[3] (CD87), respectively.

Integrins are heterodimeric membrane glycoproteins composed of noncovalently associated α and β chains (7–9). β_1 integrins include at least six distinct heterodimers (CD49a-f/CD29) that recognize ECM components including laminin, collagen, and fibronectin (7–9). On the other hand, β_3 integrins include a vitronectin receptor (CD51/CD61) and the platelet glycoprotein IIb/IIIa (CD41/CD61). These integrins have been found on tumor cell surfaces, where they participate in various aspects of tumor cell adhesion, invasion, and metastasis (1–3).

Invasion of malignant cells also requires the proteolytic degradation of extracellular materials. One key system initiating pericellular proteolysis is plasminogen activation. Plasminogen activators catalyze the activation of plasminogen to plasmin, which is a broad-spectrum protease that subsequently activates latent collagenases and elastases; this proteolytic cascade catalyzes the degradation of most extracellular proteins (4–5). The uPA is produced by invasive malignant cells (6), implanting trophoblastic cells (10) and monocytes (11). uPA binds to the cell surface uPAR, which is a GPI-linked membrane protein (12, 13). Recent studies show that uPAR expression is markedly increased on invasive tumor cells in comparison to noninvasive cells (14, 15). uPAR is apparently required for tumor cell invasion and metastasis (16, 17).

In previous studies, we and others have shown that uPAR physically interacts with the β_2 integrin CR3 on leukocyte membranes (18, 19). These interactions may participate in leukocyte invasive events. Thus, we hypothesize that β_1 and/or β_3 integrins of tumor cells may physically interact with uPAR molecules to regulate pericellular proteolytic processes. We now report that uPAR and β_1 integrins associate on tumor cells adherent to fibronectin, laminin, and vitronectin but not to polylysine and that uPAR and β_3 integrins associate on tumor cells adherent to vitronectin. Thus, integrin-uPAR interactions in tumor cell membranes may account for cytoskeletal associations of uPA (20), uPA and uPAR clustering at focal contacts (21–23), and the focusing of pericellular proteolysis at specific extracellular sites (24).

MATERIALS AND METHODS

Materials. Fructose, NADG, and poly-L-lysine were obtained from Sigma Chemical Co. (St. Louis, MO). fn and lm were obtained from Life Technologies, Inc. (Grand Island, NY). vn was purchased from Boehringer Mannheim (Indianapolis, IN). TRITC and FITC-conjugated anti-mouse IgG antibodies were obtained from Cappel-Organon Teknika Corp. (Malvern, PA).

Cell Cultures. The human fibrosarcoma cell line HT1080 (Ref. 25; CCL121; American Type Culture Collection) was obtained from the American Type Culture Collection (Bethesda, MD) and grown at 37°C in DMEM (Life Technologies, Inc.) supplemented with 10% FCS (Hyclone Laboratory, Inc., Logan, UT) and 100 μg/ml gentamicin (Life Technologies, Inc.).

Received 9/16/96; accepted 3/1/97.

The costs of publication of this article were defrayed in part by the payment of page charges. This article must therefore be hereby marked *advertisement* in accordance with 18 U.S.C. Section 1734 solely to indicate this fact.

[1] This work was supported by NIH Grant AI/CA27409 and the Research Stimulation Fund of Wayne State University (to H. R. P.) and NIH Grants CA39064 and CA42246 (to R. F. T.).

[2] To whom requests for reprints should be addressed. Phone: (313) 577-2896; Fax: (313) 577-9008.

[3] The abbreviations used are: uPAR, urokinase-type plasminogen activator receptor; ECM, extracellular matrix; GPI, glycosylphosphatidyl inositol; NADG, *N*-acetyl-D-glucosamine; fn, fibronectin; lm, laminin; vn, vitronectin; TRITC, tetramethylrhodamine isothiocyanate; mAb, monoclonal antibody; RET, resonance energy transfer; DIC, differential interference contrast.

Antibodies. Anti-uPAR mAb (anti-Mo3f, clone 3B10) was prepared as described previously (26, 27). An IgG fraction of a rabbit anti-human uPAR was obtained as described (13) for use in Western blotting procedures. HRP-conjugated goat anti-rabbit IgG Ab was obtained from Life Technologies, Inc. Goat anti-mouse IgG was obtained from Cappel-Organon Teknika Corp. (Malvern, PA).

mAb directed against integrin subunits were obtained from various sources. mAbs directed against β_1 integrin (CD29, clone P4C10; Ref. 28), α_3 subunit (CD49c, clone P1B5; Ref. 29), α_4 subunit (CD49d, clone P4G9; Ref. 30), and α_v (CD51, clone VNR147; Ref. 31) subunits were obtained from Life Technologies, Inc. Anti-β_3 (CD61, clone GPIIIA) mAb was obtained from Dako Corp. (32). Anti-α_1 (CD49a, clone TS2/7) was obtained from M. Hemler of Harvard Medical School, Boston MA (33). Anti-α_2 integrin (CD49b, clone 12F1) was obtained from V. Woods of the University of California at San Diego, La Jolla, CA (34). Rat anti-human α_5 (CD49e, clone BIIG2) was obtained from C. Damsky of the University of California at San Francisco, San Francisco, CA (35). Rat anti-human α_6 (CD49f, clone GoH3 was obtained from A. Sonnenberg of the Netherlands Cancer Institute, Amsterdam, the Netherlands (36).

Flow Cytometry. Indirect immunofluorescence was performed as described (26) using Abs directed at uPAR (26, 27), β_1, β_3, and several α subunits. Briefly, cells were incubated with a saturating concentration of Ab or an equivalent concentration of isotype-matched control Ab that was not directed against these cells at 4°C for 30 min. Cells were washed once and then incubated with a saturating concentration of FITC-conjugated polyclonal goat anti-mouse Ab (Tago, Burlingame, CA) at 4°C for 30 min. Cells were washed twice and fixed with 1% formaldehyde in PBS and then analyzed on an Epics C flow cytometer (Coulter Corporation, Hialeah, FL).

Indirect Immunofluorescence Staining for Microscopy. HT1080 tumor cells were allowed to attach for 2 h to variously coated glass coverslips. Coverslips were coated with poly-L-lysine (10 μg/ml), fn (10 μg/ml), lm (10 μg/ml), or vn (5 μg/ml) in PBS (pH 7.2) by incubating overnight at 4°C or for 2 h at 37°C, followed by extensive washing. After cells had attached and spread on these surfaces, they were fixed with 3% paraformaldehyde for 15 min at room temperature. Each coverslip was then washed several times with HBSS. Samples were then treated with murine mAb against uPAR at a concentration of 10 μg/ml for 1 h at room temperature. Isotype-matched control experiments were performed (10 μg/ml) to rule out artifactual labeling. After three washes with HBSS, the cells were incubated with TRITC-conjugated goat anti-mouse IgG (Jackson Immuno Research Labs, Inc., West Grove, PA) diluted 1:50 for 1 h at room temperature. The cells were then fixed again with 3% paraformaldehyde and blocked with 3% BSA in HBSS, followed by staining with FITC-conjugated purified mouse mAb against β_1, β_3, or α subunits for 1 h at room temperature. After three additional washes, the coverslips were inverted and mounted on slides. The stained cells were observed using epifluorescence microscopy.

Fluorescence Microscopy and Data Quantitation. Cells were observed using an axiovert inverted fluorescence microscope (Carl Zeiss, Inc., New York, NY) with mercury illumination interfaced to a Perceptics (Knoxville, TN) Biovision image processing system. RET microscopy was performed as described previously (37–39). A narrow bandpass discriminating filter set (Omega Optical, Brattleboro, VT) was used with excitation at 485/22 nm and emission at 530/30 nm for FITC and an excitation of 540/20 nm and emission of 590/30 nm for TRITC. Long-pass dichroic mirrors of 510 and 560 nm were used for FITC and TRITC, respectively. To observe RET images, the 485/22 nm narrow bandpass discriminating filter was used for excitation, and the 590/30 nm filter was used for emission. The fluorescence images were collected with an intensified charge-coupled device camera (Geniisys; Dage-MTI, Michigan City, IN). DIC photomicrographs were taken using Zeiss polarizers and a charge-coupled device camera (Model 72; Dage-MTI). RET data were quantitated with a photon counting system (Photochemical Research Associates, Inc., London, Ontario, Canada) coupled to a microscope via a Products for Research, Inc. (Danvers, MA) photomultiplier housing containing a photomultiplier tube (Hamamatsu, Bridewater, NJ) that was cooled using a Peltier system (Photochemical Research Associates) and a water circulator (Forma Scientific, Marietta, OH; Ref. 40). RET photon count rates were obtained by calculating the difference between the photon count rate of a cell and the background count rate. Approximately 60–80 cells were quantitated in each experiment. Photon count rates (photons/s) are given as the mean ± SE. *Ps* were calculated using the Stats Plus (Human Systems Dynamics, Northridge, CA) software package.

Preparation of Anti-β_1 Integrin Affinity Column. Anti-β1 mAb ascites (5 μl) or normal control mouse ascites (Sigma; 5 μl) were coupled to goat-anti-mouse IgG affinity gel (Cappel-Organon Teknika Corp.) by overnight incubation at 4°C followed by washing three times with PBS.

Immunoprecipitation and Immunoblotting. Adherent HT1080 cells were detached from flasks by Puck's EDTA solution. The cells were lysed in a lysis buffer containing 20 mM Tris (pH 8.2), 140 mM NaCl, 2 mM EDTA, 1% Brij-58 (Pierce, Rockford, IL), 5 mM iodoacetamide, 10 μg/ml aprotinin, 10 μg/ml pepstatin A, 10 μg/ml leupeptin, and 1 mM phenylmethylsulfonyl fluoride overnight at 4°C (19). In a second set of experiments, HT1080 cells were incubated with lm at 10 μg/ml ($\sim 10^7$ cells) for 2 h and then directly lysed by adding 0.5 ml of lysis buffer followed by incubation for 4 h or overnight at 4°C. The lysates were subjected to immunoprecipitation by loading lysates onto anti-β_1 affinity or control ascites (Sigma) chromatography columns overnight at 4°C, washed with lysis buffer three times, and then eluted with 2× SDS sample buffer. The chromatography columns consisted of goat anti-mouse IgG covalently coupled to Sepharose (Cappel-Organon Teknika Corp.) loaded with specific mAb or control ascites. The eluted fractions were assayed for protein content using a microassay protein kit (Bio-Rad, Hercules, CA). Samples (total protein, 50 μg) were then analyzed by SDS-PAGE and transferred to polyvinylidene difluoride membranes (Bio-Rad). The membrane was blocked for 1 h in 5% nonfat milk and stained by sequential incubation with anti-uPAR rabbit Ab or normal rabbit serum as Western blotting control, followed by horseradish peroxidase-conjugated goat anti-rabbit Ab. A chemiluminescence-enhanced detection system (ECL; Amersham Corp., Arlington Heights, IL) was used for visualization of labeled proteins.

RESULTS

Although uPAR is expressed as a GPI-linked membrane protein and thereby lacks transmembrane and cytoplasmic sequences, it is localized to adherence sites of tumor cells (21, 22). Because previous studies demonstrated physical and functional interactions between uPAR and the β_2 integrin CR3 on leukocytes (18, 19, 41–43), we hypothesized that in tumor cells lacking CR3, other integrins might physically interact with uPAR to focus pericellular proteolysis at these sites. We have tested this hypothesis using cell biological, biophysical, and biochemical methods.

Expression of uPAR and β_1 and β_3 Integrins by Fibrosarcoma Cells as Detected by Flow Cytometry. To study the possible physical associations between uPAR and β_1 or β_3 integrins on tumor cells, we first selected a tumor cell line that expresses these molecules. The expression of uPAR (CD87), β_1 (CD29), and β_3 (CD61) integrins were detected by immunofluorescence flow cytometry. Fig. 1 shows that HT1080 tumor cells express these molecules, although β_3 integrin expression is lower than β_1 integrin or uPAR expression. Furthermore, cells were positive for all α chains tested, including α_1, α_2, α_3, α_4, α_5, α_6, and α_v.

Colocalization and Physical Proximity of uPAR with β_1 and β_3 Integrins on Tumor Cells Attached to Specific Extracellular Matrix Molecules. Because several integrin subclasses participate in tumor cell metastasis and invasion (1–3), we first investigated the potential interactions of uPAR with the β_1 and β_3 integrin families. The colocalization of uPAR with β_1 or β_3 integrins on the surface of HT1080 cells was examined using indirect immunofluorescence microscopy. HT1080 cells attached to substrate-coated coverslips were fixed and then labeled with monoclonal murine anti-uPAR antibody, followed by TRITC-conjugated goat anti-murine IgG. The cells were fixed again, blocked, and then stained with FITC-conjugated murine anti-β_1 or FITC-conjugated-murine anti-β_3 integrin mAb. Fig. 2 shows uPAR and β_1 integrin staining patterns of HT1080 cells adherent to polylysine (controls)-, fn-, lm-, and vn-coated substrates. The cells were well spread on fn and vn but were mostly elongated in

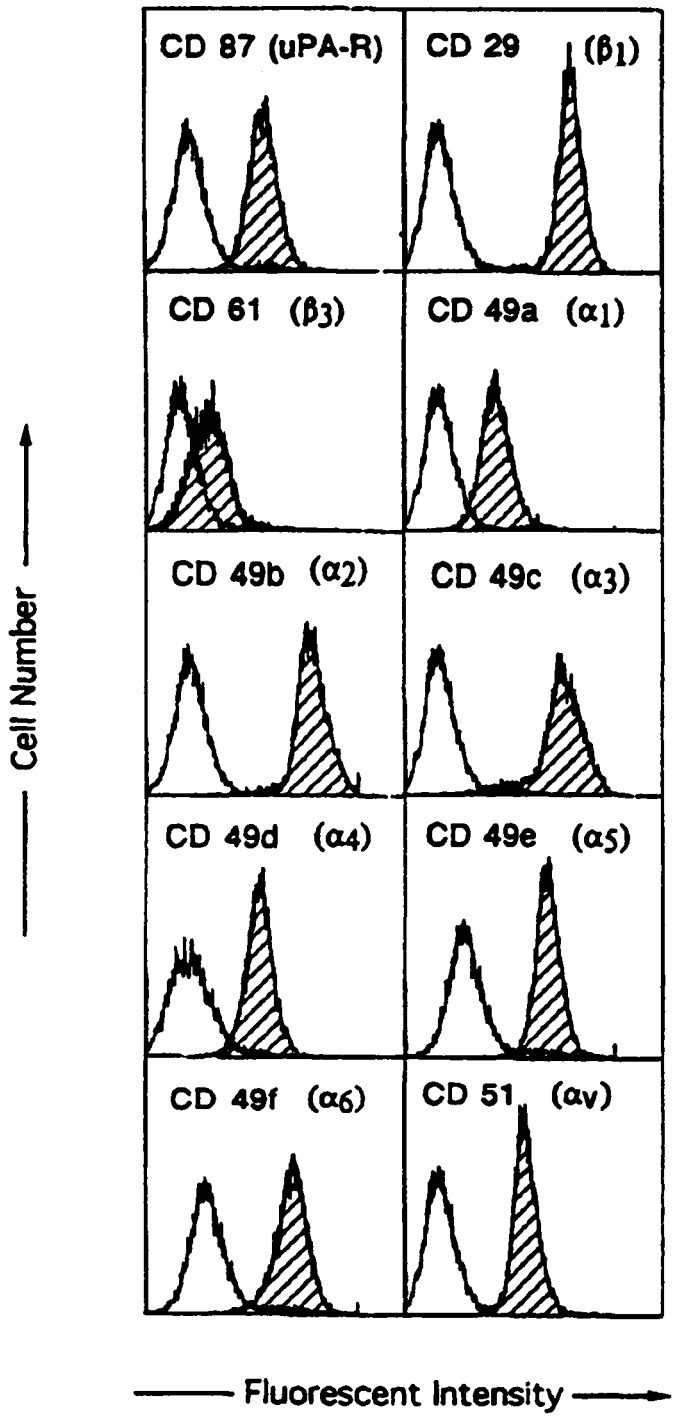

Fig. 1. Expression of uPAR, β_1, β_3, and α subunits on the tumor cell line HT1080. Indirect immunofluorescence of individual molecules on the cells was performed with either a test mAb or an isotype-matched control mAb at 4°C for 30 min. After washing, the cells were incubated with goat anti-mouse Ab at 4°C for 30 min. Cells were washed with PBS, fixed with 1% formaldehyde, and then analyzed on a Epics flow cytometry. The histograms shown represent indirect immunofluorescence with Abs directed at uPAR, β_1 integrin, β_3 integrin, and α_1, α_2, α_3, α_4, α_5, α_6, and α_v (*cross-hatched traces*), and with appropriate isotype-matched control mAbs (*open traces*).

shape on lm substrates. The staining patterns, especially at filopodia and adhesion plaques, are similar for uPAR and β_1 on cells attached to fn, lm, and vn. However, cells attached to polylysine display a spherical shape with no similarity in staining patterns. Although these colocalization experiments demonstrate that uPAR and β_1 integrins collect at the same membrane sites, they do not demonstrate molecular proximity. RET microscopy has been used to detect molecular proximity (37–39). Fig. 2, *RET*, shows RET micrographs of cells attached to polylysine-, fn-, vn-, and lm-coated surfaces. Although controls showed no RET, β_1 integrin-to-uPAR RET was qualitatively observed on cells attached to ECM components, especially at adherence sites.

A similar series of experiments was performed using anti-β_3 integrin labeling. Colocalization and RET between uPAR and β_3 integrin labels was observed on the tumor cells attached to vn, but not fn, lm, or polylysine-coated surfaces. Fig. 3 illustrates the colocalization and RET between uPAR and β_3 on HT1080 cells. Overlapping staining patterns of both adherence sites and the cell body were observed. Colocalization of uPAR and β_3 at adherence sites was found on cells attached to vn, but not to fn, lm, or polylysine. The overlap in the uniform labeling pattern, for example on cells attached to lm, is not indicative of membrane association because most receptors are uniformly distributed in membranes. Similarly, RET was observed on cells attached to vn but not on cells attached to fn, lm, or polylysine. These results contrast sharply with those described above for β_1 integrins.

Quantitative RET. To provide a quantitative measure of RET, RET intensities were measured using quantitative microfluorometry. Experiments were performed on HT1080 cells labeled with FITC-conjugated anti-β_1 or anti-β_3 integrin mAb and TRITC conjugated-anti-uPAR. Table 1 shows that the average RET photon count rate of anti-β_1 and uPAR were significantly higher on the cells attached to fn, lm, and vn than on polylysine, although no significant difference among these three ECM components was found. In contrast, significantly enhanced RET between uPAR and β_3 was observed on cells attached to vn but not fibronectin, lm, or polylysine (Table 1).

Association of uPAR with Certain α Subunits of Integrins of Tumor Cells Attached to ECM Components. To study the relationship between uPAR and individual members of the β_1 or β_3 integrin families, we performed double immunofluorescence staining experiments using mAbs against different α subunits of integrins and uPAR on tumor cells adherent to various substrates. Our results showed that α_5 colocalizes with uPAR on the cells adherent to fn (Fig. 4) and vn (Fig. 5) but not to polylysine (data not shown). Indeed, on fn-coated surfaces, all α subunits were negative except for the α_5 subunit. α_v associates with uPAR on cells adherent to vn (Fig. 5) but not to fn (Fig. 4) or polylysine (data not shown). α_3 and α_6, but not other α subunits, associate with uPAR on cells adherent to lm (Fig. 6). α_1, α_2, and α_4 have not been found to colocalize with uPAR on tumor cells adherent to any of the tested substrates (Table 2).

Inhibition of Cell Spreading and Receptor Colocalization by NADG. We have found previously that cocapping of β_2 integrins and uPAR can be inhibited by certain saccharides such as NADG and mannose but not by other saccharides such as sucrose and fructose (18). To test if similar interactions also exist between uPAR and β_1 or β_3 integrins, tumor cells were plated onto various substrates in the presence or absence of 0.15 M NADG or fructose followed by double immunofluorescence staining, as described above. Representative photomicrographs of tumor cells attached to fn (Fig. 7) or vn (Fig. 8) in the presence of NADG or fructose are shown. Colocalization and RET between uPAR and β_1 or β_3 integrins were significantly decreased in comparison with controls (Table 3). However, these saccharides had no effect on cell viability as judged by trypan blue exclusion (data not shown), as reported previously for leukocytes (18). Furthermore, in the presence of NADG, cells showed markedly decreased spreading and polarization on fn, lm, and vn.

Association of uPAR with β_1 Integrins of Tumor Cells by Immunoprecipitation and Western Blotting. To further test the physical association of uPAR and integrins within tumor cell mem-

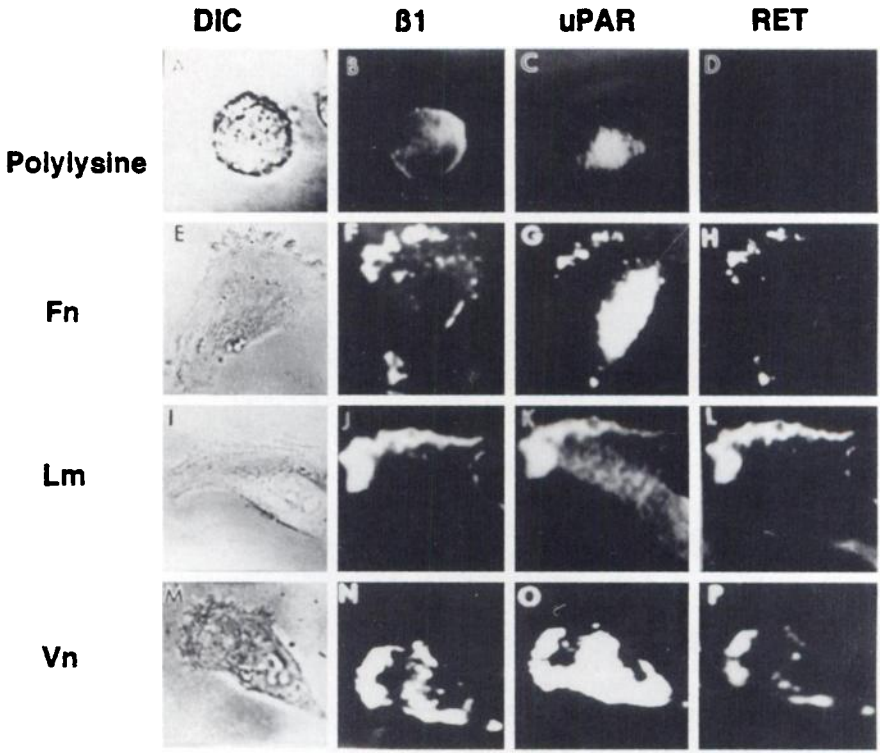

Fig. 2. Colocalization and RET of β_1 and uPAR on HT1080 tumor cells adherent to different substrates. HT1080 cells attached to various substrate-coated coverslips were examined by immunofluorescence staining. The primary antibodies included mouse FITC-conjugated anti-β_1 (*B, F, J,* and *N*) mAb and mouse anti-uPAR (*C, G, K,* and *O*) mAb. TRITC-conjugated goat-anti-mouse Ab was used as the second-step Ab. *Columns 1–4,* DIC, FITC fluorescence of anti-β_1 mAb, fluorescence of TRITC-anti-uPAR, and RET, respectively. In *row 1, A–D,* polylysine was used as substrate. In *row 2, E–H,* fn was used as substrate. In *row 3, I–L,* lm was used as substrate. In *row 4, M–P,* vn was used as substrate.

branes, we performed immunoprecipitation and Western blotting to detect the presence of uPAR in a fraction eluted from an anti-β_1 immunoaffinity chromatography column. β_1 integrins were chosen for this study because they are much more abundant on HT1080 cells than β_3 integrins (Fig. 1). The HT1080 cells were detached from flasks by Puck's EDTA to avoid the digestion of membrane proteins by trypsin. Cells were solubilized using the mild detergent Brij-58 and then subjected to immunoprecipitation, followed by Western blotting with rabbit anti-uPAR Ab and visualization with a second step reagent. Using this protocol, we detected the presence of uPAR in the precipitates of the anti-β_1 affinity column but not from normal mouse ascites column (Fig. 9), further supporting the association of uPAR with β1 integrins on tumor cells. This result is consistent with the previous observation of Bohuslav *et al.* (19), who showed the coprecipitation of uPAR with β_2 integrins from human monocytes with this method. Similar results were obtained with fn (data not shown). Interestingly,

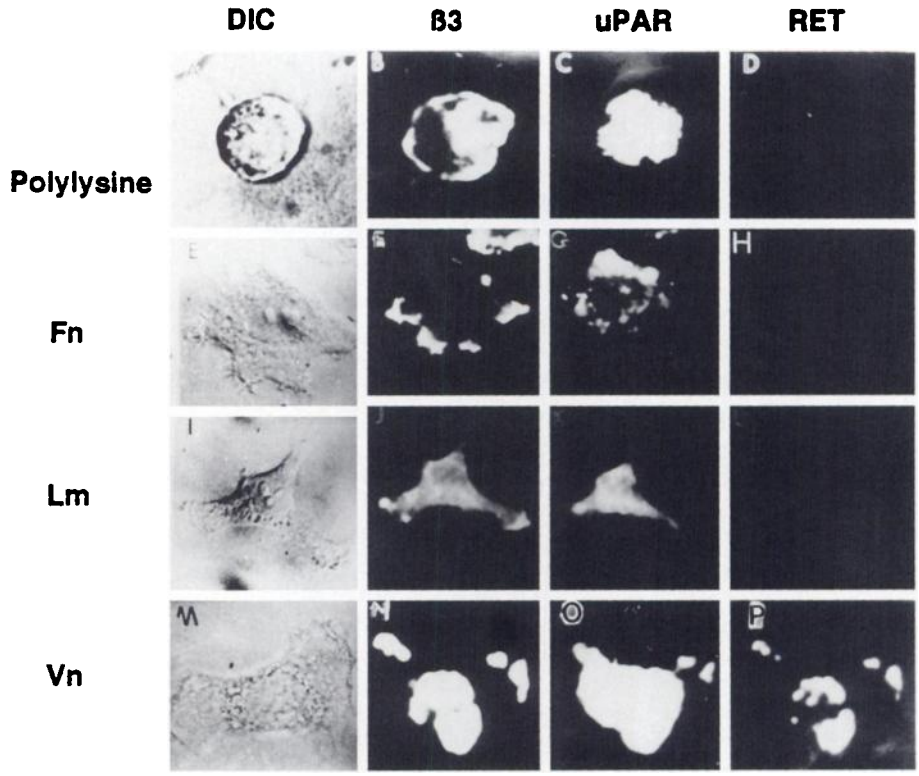

Fig. 3. Colocalization and RET of β_3 and uPAR on HT1080 tumor cells adherent to different substrates. The procedures were the same as above except that FITC-conjugated mouse anti-β_3 integrin was used instead of anti-β_1 mAb. The primary antibodies included mouse FITC-conjugated anti-β_3 (*B, F, J,* and *N*) mAb and mouse anti-uPAR (*C, G, K,* and *O*) mAb. TRITC-conjugated goat-anti-mouse Ab as second Ab. *Columns 1–4,* DIC, FITC fluorescence of anti-β3 mAb, fluorescence of TRITC-anti-uPAR, and RET, respectively. In *row 1, A–D,* polylysine was used as substrate. In *row 2, E–H,* fn was used as substrate. In *row 3, I–L,* lm used as substrate. In *row 4, M–P,* vn was used as substrate.

Table 1 *Quantitative summary of RET levels between uPAR and β_1 or β_3 integrins*

	β_1				β_3			
Substrates	N[a]	CN	RET (counts/s)	*P*	N	CN	RET (counts/s)	*P*
Polylysine	4	106	$18.7 \pm 4.2 \times 10^4$		3	100	$17.3 \pm 3.7 \times 10^4$	
fn	4	110	$48.6 \pm 5.3 \times 10^4$	<0.001	4	111	$19.4 \pm 4.1 \times 10^4$	>0.05
lm	4	102	$45.2 \pm 4.8 \times 10^4$	<0.001	3	101	$19.8 \pm 4.5 \times 10^4$	>0.05
vn	4	105	$43.1 \pm 3.8 \times 10^4$	<0.001	4	106	$42.2 \pm 4.6 \times 10^4$	<0.001

[a] N, the number of independent trials; CN, the number of cells measured.

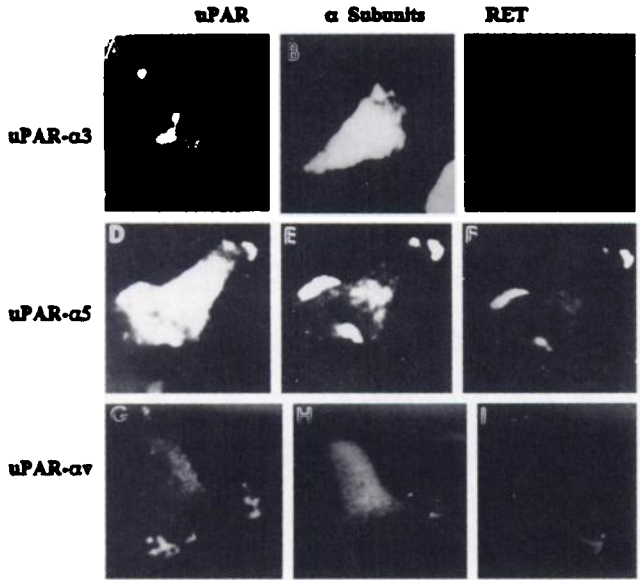

Fig. 4. Colocalization and RET of uPAR and $\alpha\beta$ integrin families on HT1080 cells adherent to fn. HT1080 cells attached to fn-coated coverslips were studied by immunofluorescence staining. Cells were labeled with mouse anti-α_1, -α_5, and -α_v subunit (*B, E,* and *H*) mAb followed by a second-step TRITC-conjugated goat-anti-mouse Ab. Cells were then labeled with FITC-conjugated anti-uPAR (*A, D,* and *G*) mAb. *Columns 1–3,* FITC fluorescence of anti-uPAR mAb, fluorescence of TRITC-anti-α subunits, and RET, respectively.

when HT1080 cells were allowed to incubate in suspension with lm (10 μg/10^7 cells) for 2 h at 37°C before cell extraction, a substantially more intense uPAR band was seen in comparison to untreated cells. This may explain why there is no detectable RET between β_1 and uPAR when HT1080 cells were adherent to polylysine, but RET between β_1 or β_3 and uPAR can be readily detected when cells adhere to ECM components.

DISCUSSION

The present study suggests that: (*a*) uPAR specifically associates with certain members of the β_1 and β_3 integrin families of membrane proteins on adherent tumor cells; and (*b*) ECM components specifically induce select integrin-uPAR associations. uPAR-to-integrin associations were especially prominent at adhesion plaques, filopodia, and pseudopodia. Evidence supporting these associations was gleaned from: (*a*) double-labeling immunofluorescence microscopy of uPAR and β_1 or β_3 integrins; (*b*) qualitative and quantitative RET microscopy; and (*c*) coimmunoprecipitation of uPAR with β_1 integrins. HT1080 tumor cells are a useful system to investigate the colocalization of uPAR with β_1/β_3 integrins because this is a nonhematopoietic tumor line that does not express β_2 integrins. Moreover, others have shown that uPAR, β_1, and β_3 integrins participate in the tumor cell invasiveness and metastatic processes (1–6, 14–17). Specificity is indicated by the facts that: (*a*) only certain members of the β_1 and β_3 integrin families are competent to interact with uPAR; and (*b*) only certain ECM-coated surfaces are competent to induce uPAR-to-integrin interactions.

Three distinct lines of evidence support the proposed uPAR-to-β_1/β_3 integrin interactions: (*a*) colocalization of uPAR with β_1 or β_3

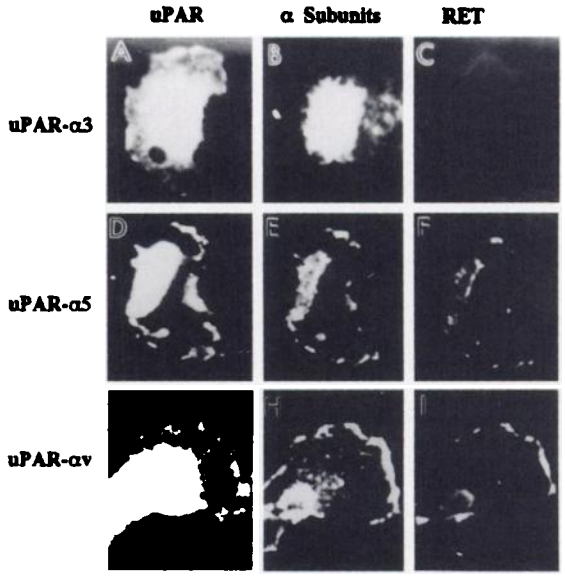

Fig. 5. Colocalization and RET of uPAR and $\alpha\beta$ integrin families on HT1080 cells adherent to vn. HT1080 cells attached to vn-coated coverslips were examined by immunofluorescence microscopy. Cells were labeled with mouse anti-α_1, -α_5, and -α_v subunit (*B, E,* and *H*) mAb followed by a TRITC-conjugated goat-anti-mouse Ab. Cells were then labeled with FITC-conjugated anti-uPAR (*A, D,* and *G*). *Columns 1–3,* FITC fluorescence of anti-uPAR mAb, fluorescence of TRITC-anti-α subunits, and RET, respectively.

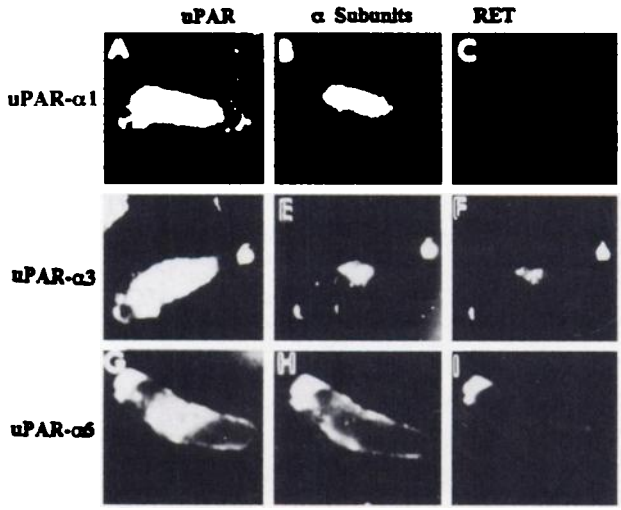

Fig. 6. Colocalization and RET of uPAR and $\alpha\beta$ integrin families on HT1080 cells adherent to lm. HT1080 cells attached to lm-coated coverslips were studied using immunofluorescence microscopy. Cells were labeled with mAb directed against α_1 (*A–C*), α_3 (*D–F*), and α_6 (*G–I*), followed by a second-step TRITC-conjugated anti-murine IgG. Cells were then labeled with anti-uPAR. *Columns 1–3,* fluorescence of anti-uPAR (*A, D,* and *G*), anti-α subunits (*B, E,* and *H*), and RET between these labels (*C, F,* and *I*).

Table 2 *Summary of α subunit specificities and coclustering/RET with uPAR on ECM components*[a]

	α subunit specificity			fn		vn		lm	
Labeling uPAR +	fn	vn	lm	Coclustering	RET	Coclustering	RET	Coclustering	RET
α_1			+	−	−	−	−	−	−
α_2			+	−	−	−	−	−	−
α_3	+		+	−	−	−	−	+	+
α_4	+			−	−	−	−	−	−
α_5	+			+	+	+	+	−	−
α_6			+	−	−	−	−	+	+
α_v	+	+		−	−	+	+	−	−

[a] These data, which summarize the morphological results shown in Figs. 4 through 6, were reproduced on three to eight separate experiments.

integrins at cell surfaces has been demonstrated by immunofluorescence microscopic analysis using specific antibodies. The presence of uPAR and β_1 and/or β_3 subunits in focal adhesion plaques suggests that they participate in adherence-related functions of HT1080 tumor cells. In contrast, colocalization was not observed on cells attached to polylysine, suggesting that ECMs trigger the colocalization of uPAR and β_1 or β_3 integrins. Furthermore, as discussed below, only certain integrin-ECM combinations were effective in promoting integrin-uPAR colocalization; (*b*) RET experiments demonstrated that, on appropriate ECM-coated surfaces, uPAR-to-β_1 or β_3 integrin molecular proximity existed. Thus, the labels were within roughly 7 nm of one another, suggesting that they are nearest neighbors within cell membranes; (*c*) using the Bohuslav *et al.* (19) procedure, we found that uPAR coimmunoprecipitated with β_1 integrins of HT1080 cells. Furthermore, to demonstrate the ECM dependence of this interaction, we added lm to HT1080 cells in suspension and found an increased level of coimmunoprecipitation, consistent with our results using attached cells. Thus, morphological, biophysical, and biochemical methods agree that uPAR is capable of associating with integrins in tumor cell membranes.

Previous studies have shown that uPA and uPAR cluster at focal contacts (21–23). Similarly, uPAR has been found to accumulate near vinculin-rich regions of membranes (20). However, because uPAR is expressed as a GPI-linked membrane protein at cell surfaces and thereby lacks transmembrane and cytosolic domains (12, 13), the mechanism responsible for restraining uPAR at adherence sites is unknown. One potential contributing factor in the accumulation of uPAR at adherence sites is interaction with ECM components. However, the NADG inhibition results would suggest that uPAR interactions with ECM components cannot completely account for uPAR clustering. Moreover, because uPAR and uPA are apparently not receptors for fn and lm, the ability of uPAR to focus at adhesion sites on these surfaces must be a property of the cell, not the surface. Our previous studies and those of others have shown that β_2 integrins physically interact with uPAR (18, 19) and other GPI-linked proteins as well (38). The present study has demonstrated that other integrins participate in uPAR clustering on tumor cells. This dramatically broadens our work to include members of the β_1 and β_3 integrin families. In contrast to our earlier work on β_2 integrins, the β_1 and β_3 integrin-to-uPAR interactions are inducible by ligation of integrins by ECM components.

The association of specific α chains with uPAR molecules was also

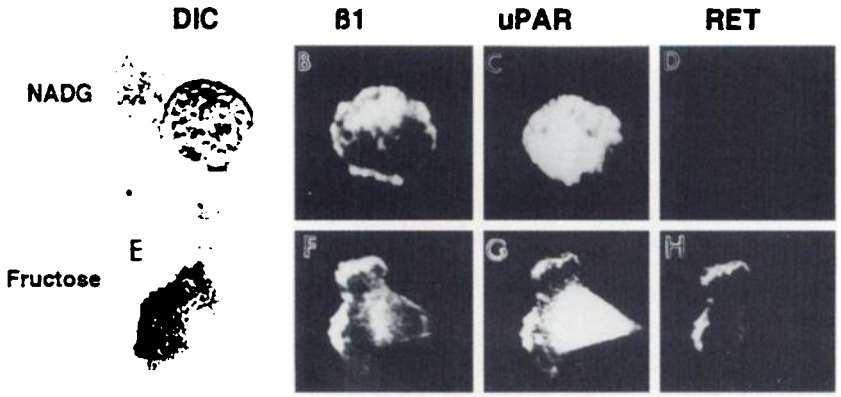

Fig. 7. Saccharide-specific inhibition of colocalization of uPAR and β_1 on HT1080 tumor cells attached to fibronectin. HT1080 tumor cells were treated with 0.15 M NADG or fructose before the cells were plated onto fibronectin. Double staining with mAb anti-uPAR and anti-β1 Ab were performed as described above. *Columns 1–4*, DIC, FITC fluorescence of anti-β_1 mAb, fluorescence of TRITC-anti-uPAR, and RET, respectively. In *row 1, A–D*, tumor cells were pretreated with 0.15 M NADG. In *row 2, E–H*, tumor cells were treated with 0.15 M fructose.

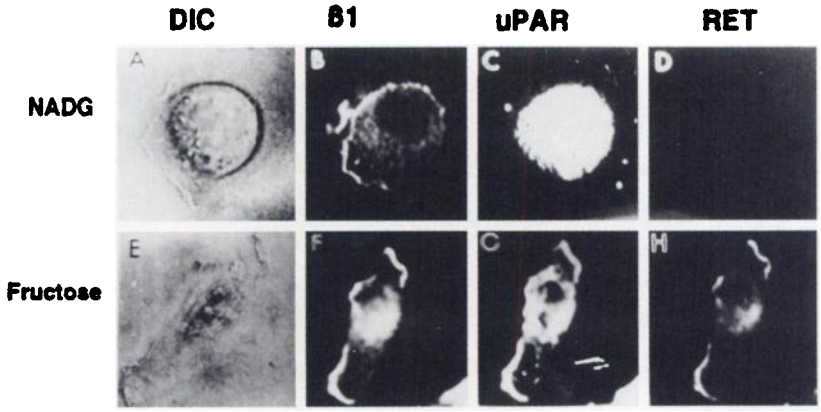

Fig. 8. Saccharide-specific inhibition of colocalization of uPAR and β_3 on tumor cells HT1080 cells attached to vn. HT1080 tumor cells were treated with 0.15 M NADG or fructose before the cells were plated onto vn. Double staining with mAb anti-uPAR and anti-β_3 Ab were performed as described above. *Columns 1–4*, DIC, FITC fluorescence of anti-β_3 mAb, fluorescence of TRITC-anti-uPAR, and RET, respectively. In row 1, *A–D*, tumor cells were pretreated with 0.15 M NADG. In *row 2, E–H*, tumor cells were treated with 0.15 M fructose.

Table 3 *Inhibition of colocalization of uPAR and $\beta_1\beta_3$ on adherent tumor cells on different substrates by NADG*

		β_1				β_3			
Substrates	inhibitors	N[a]	CN	% polarized	% RET	N	CN	% polarized	% RET
Polylysine		3	106	10	2	3	100	9	6
Polylysine	NADG	3	110	9	3	3	101	9	3
Polylysine	Fructose	3	102	11	1	3	101	8	4
fn		4	112	88	77	4	109	83	15
fn	NADG	4	115	22	13	4	110	19	18
fn	Fructose	4	110	83	79	4	107	85	16
lm		3	108	85	75	3	102	81	22
lm	NADG	3	107	20	15	3	101	21	14
lm	Fructose	3	108	86	73	3	100	79	17
vn		4	111	84	77	4	110	80	75
vn	NADG	4	112	18	11	4	105	17	18
vn	Fructose	4	109	84	78	4	107	85	76

[a] N, the number of independent trials; CN, the number of cells measured. Polarized cells are defined as those nonspherical cells exhibiting pseudopod formation and other asymmetries. RET-positive cells are defined as the percentage of cells with RET levels above background.

studied by immunofluorescence and RET microscopy. Because ECM ligand binding specificity is primarily determined by the integrins' α subunit (1–3, 7, 8), we performed immunofluorescence staining using a panel of anti-α subunit mAbs and anti-uPAR mAbs. Although $\alpha_3\beta_1$, $\alpha_4\beta_1$, and $\alpha_5\beta_1$ are fn receptors (Table 4), only the α_5 subunit, a component of the classic fn ($\alpha_5\beta_1$) receptor, was seen to colocalize with uPAR on cells adherent to fn. $\alpha_5\beta_1$ appears to be the major fn receptor and is responsible for the assembly of focal contacts, whereas $\alpha_3\beta_1$ is not (44). Interestingly, α_5 integrin subunit was also found to be associated with uPAR on the cells adherent to vn; this was surprising because α_5 does not possesses the ability to bind vn. Previous studies have reported that uPAR is a receptor for vn (45). Thus, colocalization of α_5 with uPAR may be secondary to the binding of uPAR to vn. Colocalization of α_v with uPAR was only seen on cells plated on vn but not fn, lm, or polylysine. $\alpha_3\beta_1$ and $\alpha_6\beta_1$ contribute to lm binding (1–3, 7, 8). Our colocalization studies showed that uPAR colocalized with α_3 and α_6 but not other integrin families such as α_1 and α_2 on cells adherent to lm. It might be possible that $\alpha_1\beta_1$ and $\alpha_2\beta_1$ may play a more active role in mediating cell binding to collagen.

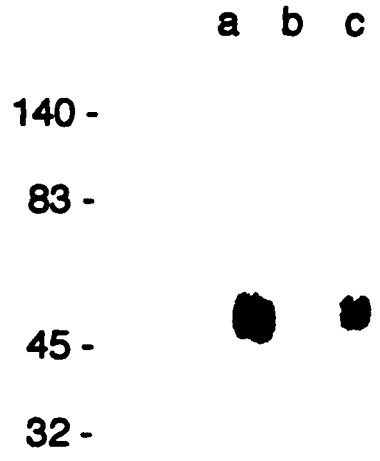

Fig. 9. Coimmunoprecipitation of uPAR with β_1 integrins. Four to 6×10^7 adherent HT1080 cells were detached from flasks with Puck's EDTA solution. Cells were extracted using a lysing buffer containing Brij-58 (19). In a parallel experiment, the same number of HT1080 tumor cells were incubated with lm (10 μg total) and then extracted as described above. β_1 integrins were precipitated by loading the cell lysates onto anti-β_1 affinity chromatography columns. The precipitates were transferred to polyvinylidene difluoride membrane and analyzed by immunoblotting with rabbit anti-uPAR or control Ab. Samples were visualized using enhanced chemiluminescence, as described in "Materials and Methods." *Lane a*, lm-treated HT1080 cells. A control lm-treated HT1080 experiment in which anti-β_1 mAb matrix was replaced with an ascites control is given in *Lane b*. *Lane c*, uPAR coimmunoprecipitates from a sample not exposed to ECM components. *Lane d*, an untreated HT1080 experiment in which the specific mAb was replaced with ascites control. Lm-treated samples consistently exhibited heavier bands after SDS-PAGE (n = 3).

Our experiments have defined the α and β subunits and ECM conditions required for integrin-uPAR associations on HT1080 cells. We have not, however, precisely defined the participating heterodimers. Nonetheless, the known subunit associations (7) and the ECM specificities noted above suggest the participation of certain heterodimers. For example, $\alpha_5\beta_1$ likely binds to uPAR on fn-coated surfaces. Similarly, $\alpha_v\beta_3$ is a vn receptor and may account for α_v-uPAR associations on vn-coated surfaces. Because α_3 specifically interacts with β_1, $\alpha_3\beta_1$ likely participates in binding uPAR on lm substrates. However, because α_6 forms heterodimers with both β_1 and β_4 subunits, it is not possible to distinguish between these two integrins at present. The integrins $\alpha_5\beta_1$, $\alpha_v\beta_3$, and $\alpha_3\beta_1$ are likely important participants in regulating the spatial locations of uPAR molecules on tumor cell membranes.

We have shown previously that certain saccharides reduce β_2 integrin interactions with uPAR (18). Earlier studies by Ross *et al.* (46, 47) showed that β_2 integrins possess a lectin-like site. Thus, to investigate the possible mechanism of interaction between uPAR and β_1 or β_3 integrins on tumor cells, receptor coclustering experiments were performed in the presence of various saccharides. The saccharide NADG, but not fructose, was found to dramatically inhibit uPAR/integrin colocalization. This suggests that saccharides of the uPA and/or uPAR molecules may participate in interreceptor interactions. Thus, it seems possible that lectin-saccharide-like interactions may also exist in uPAR-to-β_1 or -β_3 associations. This is also consistent with the observed selectivity among α subunits. However, we have not yet rigorously shown that certain saccharides act at the level of the α subunits of integrins. Nonetheless, this work suggests that anti-integrin drugs affecting inflammation may also possess antimetastatic activity.

The association of uPAR with β_1 integrins was confirmed by coimmunoprecipitation experiments. Bohuslav *et al.* (19) recently coimmunoprecipitated uPAR and β_2 integrins from Brij-58 lysates of human monocytes. Using this protocol, we detected the presence of uPAR in β_1 immunoprecipitates from tumor cells. Because the colocalization and RET of uPAR with β1 and β3 integrin were observed on the cells adherent to specific substrates but not readily detected on cells attached to polylysine or nonadherent cells, we speculate that substrates promote the association of uPAR and integrins. Tumor cells were, therefore, incubated with lm prior to cell extraction. In comparison to untreated cells,

lm-treated tumor cells exhibited increased levels of uPAR in β_1 integrin immunoprecipitates, suggesting that the association of uPAR and β_1 integrins is inducible by specific ligands, consistent with our microscopic studies. We also attempted coprecipitation of uPAR with β_3 integrins using this same protocol, but no detectable uPAR was found in β_3 immunoprecipitate. Effective β_3 integrin immunoprecipitation was confirmed by the small amount of β_3 integrin immunoprecipitated from biotin-labeled cell surfaces. The low level of β_3 integrin expression by this cell line may account for our inability to coprecipitate uPAR and β_3 integrins. Alternatively, the association of uPAR and β_3 may be less stable than uPAR-β_1 integrin associations.

Our work suggests that in addition to membrane recognition and signaling, integrins spatially regulate uPAR distribution. Thus, redistribution of the uPAR in response to ECM components provide a mechanism to achieve polarized uPAR expression and, hence, pericellular proteolysis. This allows cells to focus degradation of ECM components at specific sites that is likely required for the migration of tumor cells across tissue barriers.

REFERENCES

1. Albelda, S. M. Role of integrins and other cell adhesion molecules in tumor progression and metastasis. Lab. Invest., *68:* 4–18, 1993.
2. Giancotti, F. G., and Mainiero, F. Integrin-mediated adhesion and signaling in tumorigenesis. Biochim. Biophys. Acta, *1198:* 47–64, 1994.
3. Dedhar, S. Integrins and tumor invasion. BioEssays, *12:* 583–590, 1990.
4. Bogenmann, E., and Sones, P. A. Role of plasminogen in matrix breakdown by neoplastic cells. J. Natl. Cancer Inst., *71:* 1177–1182, 1986.
5. Bergman, B. L., Scott, R. W., Bajpai, A., Watts, S., and Baker, J. B. Inhibition of tumor cell-mediated extracellular matrix destruction by a fibroblast proteinase inhibitor, protease nexin I. Proc. Natl. Acad. Sci. USA, *83:* 996–1000, 1986.
6. Danø, K., Andreasen, P. A., Grøndahl-Hansen, J., Kristensen, P., Nielson, L. S., and Skriver, L. Plasminogen activators, tissue degradation, and cancer. Adv. Cancer Res., *44:* 139–266, 1985.
7. Hynes, R. O. Integrins: versatility, modulation, and signaling in cell adhesion. Cell, *69:* 11–25, 1992.
8. Hemler, M. E. Adhesive protein receptors on hematopoietic cells. Immunol. Today, *9:* 109–113, 1988.
9. Arnaout, M. A. Structure and function of the leukocyte adhesion molecules CD11/CD18. Blood, *75:* 1037–1050, 1990.
10. Snappino, A-P., Huarte, J., Belin, D., and Vassalli, J. D. Plasminogen activators in tissue remodeling and invasion: mRNA localization in mouse ovaries and implanting embryos. J. Cell Biol., *109:* 2471–2479, 1989.
11. Vassalli, J. D., Baccino, D., and Belin, D. Cellular binding site for the M_r 55,000 form of the human plasminogen activator, urokinase. J. Cell Biol., *100:* 86–92, 1985.
12. Ploug, M., Ronne, E., Behrendt, N., Jensen, A. L., Blasi, F., and Danø, K. Cellular receptor for urokinase plasminogen activator: carboxyl-terminal processing and membrane anchoring by glycosyl-phosphatidylinositol. J. Biol. Chem., *266:* 1926–1933, 1991.
13. Mizukami, I. F., Vinjamuri, S. D., Perini, F., Liu, D. Y., and Todd, R. F., III. Purification, biochemical characterization, and biosynthesis of the Mo3 activation antigen expressed on the plasma membrane of human mononuclear phagocytes. J. Immunol., *147:* 1331–1337, 1991.
14. Wang, H., Skibber, J., Juarez, J., and Boyd, D. Transcriptional activation of the urokinase receptor gene in invasive colon cancer. Int. J. Cancer, *58:* 650–657, 1994.
15. Hollas, W., Blasi, F., and Boyd, D. Role of the urokinase receptors in faciltating matrix invasion by cultured colon cancer. Cancer Res., *50:* 3690–3695, 1991.
16. Crowley, C. W., Cohen, R. L., Lucas, B. K., Liu, G., Shuman, M. A., and Levinson, A. D. Prevention of metastasis by inhibition of the urokinase receptor. Proc. Natl. Acad. Sci. USA, *90:* 5021–5025, 1993.
17. Ossowski, L. Invasion of connective tissue by human carcinoma cell lines: requirement for urokinase, urokinase receptor, and interstitial collagenase. Cancer Res., *52:* 6754–6760, 1994.
18. Xue, W., Kindzelskii, A. L., Todd, R. F., III, and Petty, H. R. Physical association of complement receptor type 3 and urokinase-type plasminogen activator receptor in neutrophil membranes. J. Immunol., *152:* 4630–4640, 1994.
19. Bohuslav, J., Horejsf, V., Jaansmann, C., Stockl, J., Weidle, U., Majdic, O., Bartke, I., Knapp, W., and Stockinger, H. Urokinase plasminogen activator receptor β_2-integrins, and *src*-kinases within a single receptor complex of human monocytes. J. Exp. Med., *181:* 1381–1390, 1995.
20. Hebert, C. A., and Baker, J. B. Linkage of extracellular plasminogen activator to the fibroblast cytoskeleton: colocalization of cell surface urokinase with vinculin. J. Cell Biol., *106:* 1241–1247, 1988.
21. Pollanen, J., Hedman, K., Nielsen, L. S., Danø, K., and Vaheri, A. Ultrastructural localization of plasma membrane-associated urokinase-type plasminogen activator at focal contacts. J. Cell Biol., *106:* 87–95, 1988.
22. Takahashi, K., Ikeo, K., Gojobori, T., and Tanifuji, M. Local function of urokinase receptor at the adhesion contact sites of metastatic tumor cell. Thromb. Res., *X* (Suppl.): 55–61, 1990.
23. Pollanen, J., Saksela, O., Salonen, E-M., Andreasen, P., Nielsen, L., Danø, K., and Vaheri, A. Distinct localizations of urokinase-type plasminogen activator and its type 1 inhibitor under cultured human fibroblasts and sarcoma cells. J. Cell Biol., *104:* 1085–1096, 1987.
24. Kindzelskii, A. L., Ahmad, I., Anderson, D., Zhou, M-J., Haugland, R. P., Mizukami, I., Gyetko, M., Todd, R. F., III, and Petty, H. R. Urokinase-type plasminogen activator receptors (uPAR) focus substrate proteolysis by neutrophils and tumor cells. FASEB J., *10:* A1333, 1996.
25. Laug, W. E., Wang, K., Mundi, R., Rideout, W., Kruithof, E. K. O., and Bogenmann, E. Clonal variation of expression of the genes coding for plasminogen activators, their inhibitors and the urokinase receptor in HT1080 sarcoma cells. Int. J. Cancer, *52:* 298–304, 1992.
26. Mizukami, I. F., Vinjamuri, S. D., Trochelman, R. D., and Todd, R. F., III. A structural characterization of the Mo3 activation antigen expressed on the plasma membrane of human mononuclear phagocytes. J. Immunol., *144:* 1841–1848, 1991.
27. Min, H. Y., Semnani, R., Mizukami, I. F., Watt, K., Todd, R. F., III, and Liu, D. Y. cDNA for Mo3, a monocyte activation antigen, encodes the human receptor for urokinase plasminogen activator. J. Immunol., *148:* 3636–3642, 1992.
28. Wayner, E. A., Orlando, R. A., and Cheresh, D. A. Integrins $\alpha_v\beta_3$ and $\alpha_v\beta_5$ contribute to cell attachment to vitronectin but differentially distribute on the cell surface. J. Cell. Biol., *113:* 919–929, 1991.
29. Wayner, E. A., Carter, W. G., Piotrowicz, R. S., and Kunicki, T. J. The function of multiple extracellular matrix receptors in mediating cell adhesion to extracellular matrix: preparation of monoclonal antibodies to the fibronectin receptor that specifically inhibit cell adhesion to fibronectin and react with platelet glycoproteins Ic-IIa. J. Cell. Biol., *107:* 1881–1891, 1988.
30. Wayner, E. A., Carcia-Pardo, A., Humphries, M. J., McDonald, J. A., and Carter, W. G. Identification and characterization of the T lymphocyte adhesion receptor for an alternative cell attachment domain (CS-1) in plasma fibronectin. J. Cell. Biol., *109:* 1321–1330, 1989.
31. Freed, E., Gailit, J., van der Geer, P., Ruoslahti, E., and Hunter, T. A novel integrin β subunit is associated with the vitronectin receptor α subunit (α_v) in a human osteosarcoma cell line and is a substrate for protein kinase C. EMBO J., *8:* 2955–2965, 1989.
32. Gatter, R. C., Gordell, J. G., Turley, H., Heryel, A., Kieffer, N., Anstee, D. J., and Mason, D. Y. The immunohistological detection of platelets megakaryocytes and thrombi in routinely processed specimens. Histopathology, *13:* 257–267, 1988.
33. Hemler, M. E., Sanchez-Madrid, F., Flotte, T. J., Krensky, A. M., Burokoff, S. J., Bhan, A. K., Springer, T. A., and Strominger, J. L. Glycoproteins of 210,000 and 130,000 M.W. on activated T cells: cell distribution and antigenic relation to components on resting cells and T cells lines. J. Immunol., *132:* 3011–3017, 1984.
34. Pischel, K. D., Hemler, M. E., Huang, C., Blueatein, H. G., and Woods, V. L. Use of the monoclonal antibody 12F1 to characterize the differentiation antigen VLA-2. J. Immunol., *138:* 226–233, 1987.
35. Brown, D. J., Phillips, D. R., Damsky, C. H., and Charo, I. F. Synthesis and expression of the fibroblast fibronectin receptor in human monocytes. J. Clin. Invest., *84:* 366–370, 1989.
36. Sonnenberg, A., Janasen, H., Hogervorst, F., Calofat, J., and Hilgers, J. A. Complex of platelet glycoproteins Ic and IIa identified by a rat monoclonal antibody. J. Biol. Chem., *262:* 10376–10383, 1987.
37. Uster, P. S., and Pagano, R. E. Resonance energy transfer microscopy: observations of membrane-bound fluorescent probes in model membranes and in living cells. J. Cell Biol., *103:* 1221–1234, 1986.
38. Zhou, M-J., Todd, R. F., III, and Petty, H. R. Detection of transmembrane linkage between immunoglobulin or complement receptors and the neutrophil's cortical microfilaments by resonance energy transfer microscopy. J. Mol. Biol., *218:* 263–268, 1991.
39. Zhou, M-J., Poo, H., Todd, R. F., III, and Petty, H. R. Surface bound immune complexes trigger transmembrane proximity between complement receptor type 3 and the neutrophil's cortical microfilaments. J. Immunol., *148:* 3550–3553, 1992.
40. Maher, R. J., Cao, D., Boxer, L. A., and Petty, H. R. Simultaneous calcium-dependent delivery of neutrophil lactoferrin and reactive oxygen metabolites to erythrocyte targets: evidence supporting granule-dependent triggering of superoxide deposition. J. Cell. Physiol., *156:* 226–234, 1993.
41. Cao, D., Mizukami, I. F., Garni-Wagner, B. A., Kindzelskii, A. L., Todd, R. F., III, Boxer, L. A., and Petty, H. R. Human urokinase-type plasminogen activator primes neutrophils for superoxide anion release: possible roles of complement receptor type 3 and calcium. J. Immunol., *154:* 1817–1829, 1995.
42. Sitrin, R. G., Todd, R. F., Petty, H. R., Brock, T. G., Shollenberger, S. B., Albrecht, E., and Gyetko, M. R. The urokinase receptor (CD87) facilitates CD11b/CD18-mediated adhesion of human monocytes. J. Clin. Invest., *97:* 1942–1951, 1996.
43. Petty, H. R., and Todd, R. F. Integrins as promiscuous signal transduction devices. Immunol. Today, *17:* 209–212, 1996.
44. Simon, K. O., and Burridge, K. Interactions between integrins and the cytoskeleton: structure and regulation. *In:* D. A. Cheresh and R. P. Mecham (eds.), Integrins: Molecular and Biological Response to the Extracellular Matrix, pp. 49–78. New York: Academic Press, Inc., 1994.
45. Wei, Y., Waltz, D. A., Rao, N., Drummond, R. J., Rosenberg, S., and Chapman, H. A. Identification of the urokinase receptor as an adhesion receptor for vitronectin. J. Biol. Chem., *269:* 32380–32388, 1994.
46. Ross, G. D., Cain, J. A., and Lachmann, P. J. Membrane complement receptor type three (CR3) has lectin-like properties analogous to bovine conglutinin and functions as a receptor for zymosan and rabbit erythrocytes as well as a receptor for iC3b. J. Immunol., *134:* 3307–3315, 1985.
47. Ross, G. D., Cain, J. A., Myones, B. L., Newman, S. L., and Lachmann, P. J. Specificity of membrane complement receptor type three (CR3) for β-glucans. Complement, *4:* 61–74, 1987.